

See discussions, stats, and author profiles for this publication at: <https://www.researchgate.net/publication/304498202>

Intensification and poleward shift of subtropical western boundary currents in a warming climate

Article *in* Journal of Geophysical Research: Oceans · June 2016

DOI: 10.1002/2015JC011513

READS

380

6 authors, including:



G. Lohmann

Alfred Wegener Institute Helmholtz Centre f...

328 PUBLICATIONS 5,241 CITATIONS

[SEE PROFILE](#)



Wei Wei

Alfred Wegener Institute Helmholtz Centre f...

14 PUBLICATIONS 152 CITATIONS

[SEE PROFILE](#)



Mihai Dima

University of Bucharest

33 PUBLICATIONS 872 CITATIONS

[SEE PROFILE](#)



Monica Ionita

Alfred Wegener Institute Helmholtz Centre f...

47 PUBLICATIONS 180 CITATIONS

[SEE PROFILE](#)

Intensification and Poleward Shift of Subtropical Western Boundary Currents in a warming climate

Hu Yang¹, Gerrit Lohmann^{1,2}, Wei Wei¹, Mihai Dima^{1,3}, Monica Ionita¹, Jiping Liu⁴

¹ Alfred Wegener Institute, Helmholtz Centre for Polar and Marine Research, Bremerhaven, Germany

² Department of Environmental Physics, University of Bremen, Bremen, Germany

³ Faculty of Physics, University of Bucharest, Bucharest, Romania

⁴ Department of Atmospheric and Environmental Sciences, University at Albany, State University of New York, New York,
USA

Key Points:

- WBCs are strengthening and shifting towards poles under global warming.
- Three types of independent data sets are included.
- Several coupled parameters are used to identify the WBCs dynamics.

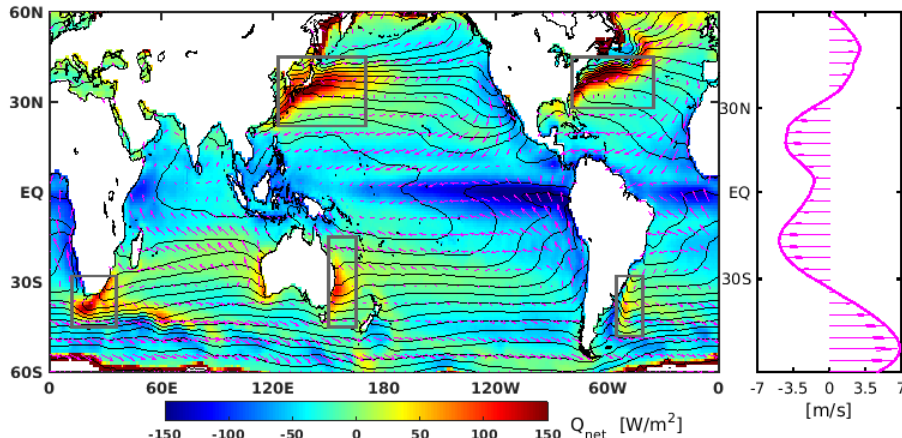
13 **Abstract**

14 A significant increase in sea surface temperature (SST) is observed over the mid-latitude west-
 15 ern boundary currents (WBCs) during the past century. However, the mechanism for this phe-
 16 nomenon remains poorly understood due to limited observations. In the present paper, sev-
 17 eral coupled parameters (i.e., sea surface temperature (SST), ocean surface heat fluxes, ocean
 18 water velocity, ocean surface winds and sea level pressure (SLP)) are analyzed to identify the
 19 dynamic changes of the WBCs. Three types of independent data sets are used, including re-
 20 analysis products, satellite-blended observations and climate model outputs from the fifth phase
 21 of the Climate Model Intercomparison Project (CMIP5). Based on these broad ranges of data,
 22 we find that the WBCs (except the Gulf Stream) are intensifying and shifting toward the poles
 23 as long-term effects of global warming. An intensification and poleward shift of near-surface
 24 ocean winds, attributed to positive annular mode-like trends, are proposed to be the forcing
 25 of such dynamic changes. In contrast to the other WBCs, the Gulf Stream is expected to be
 26 weaker under global warming, which is most likely related to a weakening of the Atlantic Merid-
 27 ional Overturning Circulation (AMOC). However, we also notice that the natural variations
 28 of WBCs might conceal the long-term effect of global warming in the available observational
 29 data sets, especially over the Northern Hemisphere. Therefore, long-term observations or proxy
 30 data are necessary to further evaluate the dynamics of the WBCs.

31 **1 Introduction**

32 The subtropical western boundary currents (WBCs), including the Kuroshio Current, the
 33 Gulf Stream, the Brazil Current, the East Australian Current and the Agulhas Current, are the
 34 western branches of the subtropical gyres. They are characterized by fast ocean velocities, sharp
 35 sea surface temperature (SST) fronts and intensive ocean heat loss. The strength and routes
 36 of WBCs have a broad impact on the weather and climate over the adjacent mainland. For in-
 37 stance, WBCs regions favor the formation of severe storms [Kelly *et al.*, 1996; Inatsu *et al.*,
 38 2002; Taguchi *et al.*, 2009; Cronin *et al.*, 2010], while the poleward ocean heat transport by
 39 the WBCs contributes to the global heat balance [Colling, 2001].

40 In recent years, there has been an increasing interest in the variability of WBCs under
 41 global warming. Deser *et al.* [1999] suggested that there has been a decadal intensification of
 42 Kuroshio Current during the 1970-1980 period due to a decadal variation in wind stress curl,
 43 whereas Sato *et al.* [2006] and Sakamoto *et al.* [2005] projected a stronger Kuroshio Current
 44 in response to global warming according to a high-resolution coupled atmosphere-ocean cli-
 45 mate model. Curry and McCartney [2001] found that the transport of the Gulf Stream has in-
 46 tensified after the 1960s, which is attributed to a stronger North Atlantic Oscillation. In agree-
 47 ment with Curry and McCartney [2001], an increase in the storm frequency has also been recorded
 48 in extreme turbulent heat fluxes events over the Gulf Stream [Shaman *et al.*, 2010]. For the
 49 South Pacific Ocean, Qiu and Chen [2006] and Roemmich *et al.* [2007] suggested that the 1990s
 50 decadal increase in sea surface height over the subtropical western basin of the South Pacific
 51 is related to a spin-up of the local subtropical ocean gyres. Based on long-term temperature
 52 and salinity observations from an ocean station off eastern Tasmania, Ridgway [2007] demon-
 53 strated that the East Australian Current has increased over the past 60 years. Based on repeated
 54 high-density XBT transects, CTD survey and satellite altimetry, Ridgway *et al.* [2008] also found
 55 a strengthening of the East Australian Current in the 1990s. Regarding the South Atlantic Ocean,
 56 Goni *et al.* [2011] observed a southward shift of the Brazil Current during 1993-2008 using
 57 satellite-derived sea height anomaly and sea surface temperature (SST). Over the Indian Ocean,
 58 the Agulhas leakage was reported to have increased due to latitudinal shifts in the Southern
 59 Hemisphere Westerlies [Biastoch *et al.*, 2009]. In addition, modelling studies indicate ocean
 60 circulation changes over the Southern Hemisphere in response to a positive trend of the South-
 61 ern Annular Mode [Hall and Visbeck, 2002; Cai *et al.*, 2005; Sen Gupta and England, 2006;
 62 Cai, 2006; Fyse and Saenko, 2006; Sen Gupta *et al.*, 2009]. These studies consistently show
 63 that the Southern Hemisphere subtropical gyres do shift southward as a consequence of a pos-
 64 itive Southern Annular Mode.



82 **Figure 1.** Left: Distribution of climatological Q_{net} (shaded, positive upward), SST (black contours, con-
 83 tour interval is 2 K) and near-surface ocean winds (pink arrows). Right: Zonally averaged near-surface ocean
 84 zonal wind speeds (positive westerly). Q_{net} is from the OAFlux/ISCCP data set; SST is from the HadISST1
 85 data set; near-surface ocean winds are based on the NCEP/NCAR. The overlapping periods 1984–2009 are
 86 selected to derive the climatological conditions.

65 Besides these studies focusing on individual branches of the WBCs, recent work sug-
 66 gests that the change over the WBCs is likely to be a global phenomenon over all ocean basins
 67 [Wu *et al.*, 2012; Yang *et al.*, 2016]. Based on multiple SST data sets, Wu *et al.* [2012] reported
 68 that a stronger warming trend occurred over the WBCs during the past century. They proposed
 69 that a synchronous poleward shift and/or intensification of WBCs were associated with the iden-
 70 tified ocean surface warming [Wu *et al.*, 2012]. Yang *et al.* [2016] found that the ocean sur-
 71 face heat loss over the subtropical expansions of WBCs have increased, suggesting a stronger
 72 WBCs in the past half century. However, the confidence in WBCs dynamics changes is con-
 73 troversy due to the uncertainties and limitations of the data sets [Brunke *et al.*, 2002; L'Ecuyer
 74 and Stephens, 2003; Van de Poll *et al.*, 2006; Gulev *et al.*, 2007; Krueger *et al.*, 2013; Dee *et al.*,
 75 2014]. Here, we use a wide range of independent datasets and metrics to evaluate the dynamic
 76 changes of WBCs.

77 WBCs transport large quantities of heat from the tropics to mid and high latitudes, and
 78 much of the heat is released along the routes of these currents. As shown in Fig. 1, the me-
 79 andering of WBCs can be clearly captured by the upward ocean surface heat flux. Following
 80 this idea, ocean surface heat flux is used as the main metric to identify the dynamic changes
 81 of WBCs.

82 The available ocean surface heat fluxes data sets have several potential sources of un-
 83 certainty (e.g., uncertainty in the flux computation algorithms, sampling issues, instrument bi-
 84 ases, changing observation systems) [Brunke *et al.*, 2002; L'Ecuyer and Stephens, 2003; Van de
 85 Poll *et al.*, 2006; Gulev *et al.*, 2007]. Each data set has its own advantages and weaknesses.
 86 Satellite-blended records give observations with excellent spatial/temporal sampling, but they
 87 suffer from a lack of temporal coverage, which is insufficient to examine the long-term vari-
 88 ability. Reconstructed and reanalysis products cover longer periods by synthesizing a variety
 89 of observations. However, the changing mix of observations can introduce spurious variabil-
 90 ity and trends into the output [Dee *et al.*, 2014]. The coupled general circulation models (CGCM)
 91 have the ability to simulate the Earth's climate over hundreds of years with consistent phys-
 92 ical behaviors, but their performance on reproducing the climate variability is still under eval-
 93 uation [Refsgaard *et al.*, 2014; Bellucci *et al.*, 2014]. For achieving reliable and comprehen-
 94 95 96 97 98

113

Table 1. List of data sets used in this study

Data Type	Data Name	Periods	References
Reconstructed	HadISST	1870-2014	<i>Rayner et al.</i> [2003]
Reconstructed	HadCRUT4	1850-2014	<i>Morice et al.</i> [2012]
Satellite-blended	OISSTv2	1982-2014	<i>Reynolds et al.</i> [2002]
Satellite-blended	OAFlux/ISCCP	1983-2009	<i>Rossow and Schiffer</i> [1991]; <i>Yu et al.</i> [2008]
Atmospheric Reanalyses	NCEP/NCAR	1948-2014	<i>Kalnay et al.</i> [1996]
Atmospheric Reanalyses	ERA40	1958-2001	<i>Uppala et al.</i> [2005]
Atmospheric Reanalyses	20CRv2	1871-2012	<i>Compo et al.</i> [2006, 2011]
Atmospheric Reanalyses	ERA-20C	1900-2010	<i>Poli et al.</i> [2016]
Ocean Reanalyses	ORA-S4	1958-2009	<i>Balmaseda et al.</i> [2013]
Ocean Reanalyses	SODA2.2.0	1948-2008	<i>Carton and Giese</i> [2008]
Ocean Reanalyses	GECCO	1952-2001	<i>Köhl and Stammer</i> [2008]
Ocean Reanalyses	GECCO2	1948-2014	<i>Köhl</i> [2015]
Climate Model	CMIP5/historical	1850-2005	<i>Taylor et al.</i> [2012]
Climate Model	CMIP5/RCP4.5	2006-2300	<i>Taylor et al.</i> [2012]

99 sive results, all three types of heat flux data sets mentioned above are included here. More-
 100 over, the results based on sea surface heat flux will also be cross-validated by the ocean ve-
 101 locity fields and ocean surface winds. Since the reliability of the data sets before the 1950s
 102 is still a subject of controversy [Krueger et al., 2013], we focus our analysis on the period af-
 103 ter 1958. The paper is organized as follows. In section 2, the data sets and methods used are
 104 briefly introduced. Section 3 presents the observed and simulated dynamic changes of the WBCs.
 105 The physical mechanism responsible for these changes is investigated in section 4. Discus-
 106 sion and conclusions are given in sections 5 and 6, respectively.

107 2 Data and Methodology

108 All the data sets used in this paper are listed in Table 1. The reconstructed SST from
 109 the Hadley Centre Global Sea Ice and Sea Surface Temperature v1 (HadISST1, 1870-2013)
 110 [Rayner et al., 2003] is used to compute the SST indices of individual WBCs. Besides, the time
 111 series of near surface temperature from the HadCRUT4 (1850-2013) [Morice et al., 2012] is
 112 utilized to represent the signal of global warming.

114 Besides, two satellite-blended data sets are applied to identify the dynamic changes of
 115 WBCs. They are the SST from the Optimum Interpolation SST Analysis Version 2 (OISSTv2,
 116 1982-2013) [Reynolds et al., 2002], and the net surface heat flux (Q_{net} , sum of the radiative
 117 and turbulent heat fluxes) from the Objectively Analyzed Air-sea Fluxes and the International
 118 Satellite Cloud Climatology Project (OAFlux/ISCCP, 1983-2009) [Rossow and Schiffer, 1991;
 119 Yu et al., 2008].

120 Moreover, two atmospheric reanalyses and four ocean reanalyses data sets are included,
 121 namely the National Centers for Environmental Prediction / National Center for Atmospheric
 122 Research reanalysis (NCEP/NCAR, 1948-2013) [Kalnay et al., 1996], the European Centre for
 123 Medium-Range Weather Forecasts 40-year Reanalysis (ERA40, 1958-2001) [Uppala et al., 2005],
 124 the European Centre for Medium-Range Weather Forecasts ocean reanalysis system 4 (ORA-
 125 S4, 1958-2009) [Balmaseda et al., 2013], the Simple Ocean Data Assimilation (SODA2.2.0,
 126 1948-2008) [Carton and Giese, 2008], and the German partner of the consortium for Estimat-
 127 ing the Circulation and Climate of the Ocean (GECCO, 1952-2001, and GECCO2, 1948-2014)
 128 [Köhl and Stammer, 2008; Köhl, 2015].

Furthermore, the *historical* and Representative Concentration Pathway 4.5 (*RCP4.5*) simulations from the fifth phase of the Climate Model Intercomparison Project (CMIP5) [Taylor *et al.*, 2012] are used as well. 27 climate models are included to obtain the ensemble trends based on both *historical* and *RCP4.5* simulations. Detailed information on the models we used here is summarized in Table 2.

Additionally, the results from the Twentieth Century Reanalysis (20CRv2) [Compo *et al.*, 2006, 2011] and the ECMWF's first atmospheric reanalysis of the 20th century (ERA-20C) [Poli *et al.*, 2016] are provided in the supplementary materials to further validate our results.

The data sets used in the present paper cover different time periods. For the reanalysis data sets, the overlapping period from 1958 to 2001 is selected. We examine the same time period (1958-2001) for the CMIP5 *historical* simulations and for the *RCP4.5* simulations the time period of 2006-2100. As the CMIP5 models have different spatial resolutions and numbers of ensemble members, the trends in each CGCMs from the first ensemble member (named *r1i1p1*) [Taylor *et al.*, 2010] are computed first. Then the trends are re-gridded onto a regular $1^\circ \times 1^\circ$ latitude-longitude grid using bilinear interpolation. Finally, they are averaged over all the corresponding simulations to get the multi-model ensemble trends. As the satellite-blended data sets cover relative short periods, the whole available time interval is utilized.

3 Dynamic changes of WBCs

3.1 Results from observations

Fig. 2 shows the SST indices of the five WBCs after removing the globally averaged SST anomaly. Positive trends are observed, indicating that the ocean surface warming over the WBCs is outpacing other regions. Moreover, the SST indices of WBCs share similarities with the global warming signal. These features raise the question as to whether the strength of WBCs is affected by the global warming. It is also noticed that the SST indices of WBCs have strong decadal variations, especially for the Kuroshio Current and the Gulf Stream.

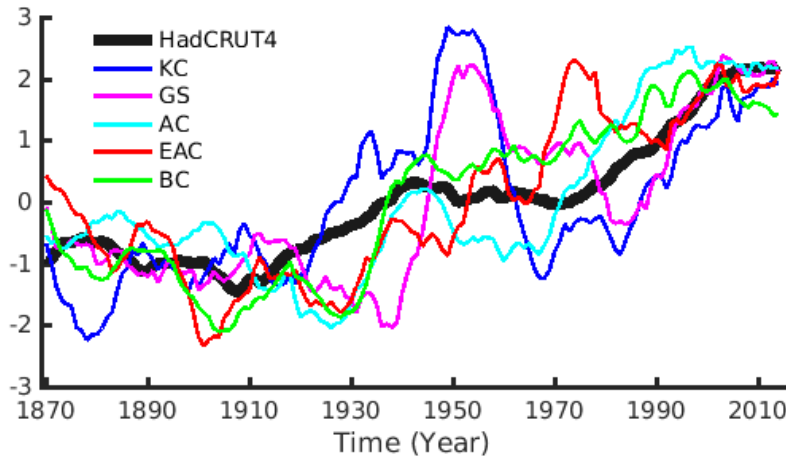
The trends in SST and Q_{net} (positive-upward) are depicted in Figs. 3 and 4 (shading). The corresponding climatology values (contours) are also presented to locate the background routes of the WBCs.

The magnitudes and distributions of SST and Q_{net} trends reveal discrepancies among different data sets over different time periods. In a relative short period of time, the satellite-blended data sets (OISSTv2 and OAFlux/ISCPP) mainly capture the signal of decadal climate variability, i.e., a negative phase of Pacific Decadal Oscillation [Mantua *et al.*, 1997] over the Pacific Ocean, and a positive phase of Atlantic Multidecadal Oscillation [Schlesinger and Ramanukuty, 1994] over the Atlantic Ocean. Over a longer time scale, an overwhelming ocean surface warming is observed in the reanalysis data sets. Despite these discrepancies, consistent features emerge over the mid-latitude expansions of the WBCs with substantial increase in both SST and Q_{net} . Such trends occur not only over individual WBCs, but for WBCs within all ocean basins. From a perspective of ocean-atmosphere heat balance, increased SST accompanied by enhanced ocean surface heat loss indicates that the ocean surface warming is not caused by the atmospheric forcing, but by an intensified ocean heat transport though the WBCs.

With respect to the regional features, we find that the trends are asymmetrical over different flanks of the WBCs. Both NCEP and ERA40 show a stronger increase in SST and Q_{net} at the polar flanks of the Gulf Stream, the Brazil Current, the East Australian Current and the Agulhas Current. While, decreases or relative weaker increases in SST and Q_{net} present themselves over the equator flanks of the above currents. The asymmetrical pattern reveals that the positions of the SST gradients and the high Q_{net} , induced by WBCs, are shifting towards the polar regions. However, one clear exception is found over the North Pacific Ocean, i.e., the Kuroshio Current, which experiences a stronger positive trend in Q_{net} at the equatorial flank

Table 2. List of CMIP5 models used in this study

Model Name	Institutions
BCC-CSM1-1	Beijing Climate Center, China Meteorological Administration
BNU-ESM	College of Global Change and Earth System Science, Beijing Normal University
CanESM2	Canadian Centre for Climate Modelling and Analysis
CCSM4	National Center for Atmospheric Research
CESM1-BGC	National Science Foundation, Department of Energy, National Center for Atmospheric Research
CESM1-CAM5	National Science Foundation, Department of Energy, National Center for Atmospheric Research
CNRM-CM5	Centre National de Recherches Meteorologiques / Centre Europeen de Recherche et Formation Avancees en Calcul Scientifique
CSIRO-Mk3.6.0	Commonwealth Scientific and Industrial Research Organisation in collaboration with the Queensland Climate Change Centre of Excellence
FGOALS-g2	LASG, Institute of Atmospheric Physics, Chinese Academy of Sciences; and CESS, Tsinghua University
FIO-ESM	The First Institute of Oceanography, SOA, China
GFDL-CM3	Geophysical Fluid Dynamics Laboratory
GFDL-ESM2G	Geophysical Fluid Dynamics Laboratory
GFDL-ESM2M	Geophysical Fluid Dynamics Laboratory
GISS-E2-H	NASA Goddard Institute for Space Studies
GISS-E2-R	NASA Goddard Institute for Space Studies
HadGEM2-CC	Met Office Hadley Centre
HadGEM2-ES	Met Office Hadley Centre and Instituto Nacional de Pesquisas Espaciais
INM-CM4	Institute for Numerical Mathematics
IPSL-CM5A-MR	Institut Pierre-Simon Laplace
IPSL-CM5B-LR	Institut Pierre-Simon Laplace
MIROC-ESM-CHEM	Japan Agency for Marine-Earth Science and Technology, Atmosphere and Ocean Research Institute (The University of Tokyo), and National Institute for Environmental Studies
MIROC5	Atmosphere and Ocean Research Institute (The University of Tokyo), National Institute for Environmental Studies, and Japan Agency for Marine-Earth Science and Technology
MPI-ESM-LR	Max Planck Institute for Meteorology (MPI-M)
MPI-ESM-MR	Max Planck Institute for Meteorology (MPI-M)
MRI-CGCM3	Meteorological Research Institute
NorESM1-ME	Norwegian Climate Centre
NorESM1-M	Norwegian Climate Centre

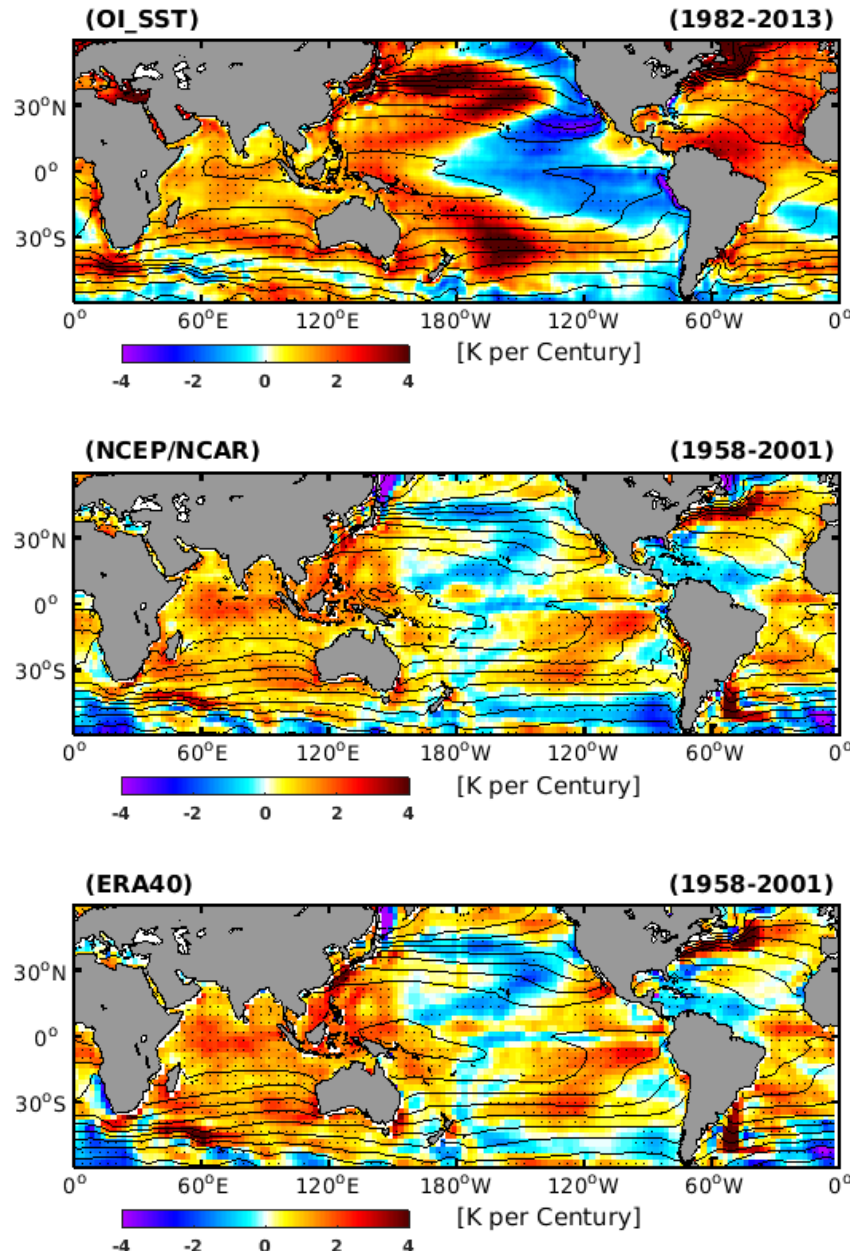


149 **Figure 2.** SST indices of WBCs (thin color line) and signal of global warming (HadCRUT4, thick black
 150 line). All indices are standardized after applying an 11-year running mean. SST indices of WBCs are ex-
 151 tracted using the following approach: Firstly, regional mean SST indices are calculated over individual WBCs
 152 (as shown with grey rectangles in Fig. 1, i.e., Kuroshio Current (KC), $123^{\circ}E - 170^{\circ}E, 22^{\circ}N - 45^{\circ}N$;
 153 Gulf Stream (GS), $79^{\circ}W - 35^{\circ}W, 28^{\circ}N - 45^{\circ}N$; Eastern Australian Current (EAC), $150^{\circ}E - 165^{\circ}E,$
 154 $15^{\circ}S - 45^{\circ}S$; Brazil Current (BC), $55^{\circ}W - 41^{\circ}W, 48^{\circ}S - 28^{\circ}S$; Agulhas Current (AC), $12^{\circ}E - 36^{\circ}E,$
 155 $45^{\circ}S - 28^{\circ}S$). Then, the globally averaged SST anomaly is removed from the SST indices of individual
 156 WBCs.

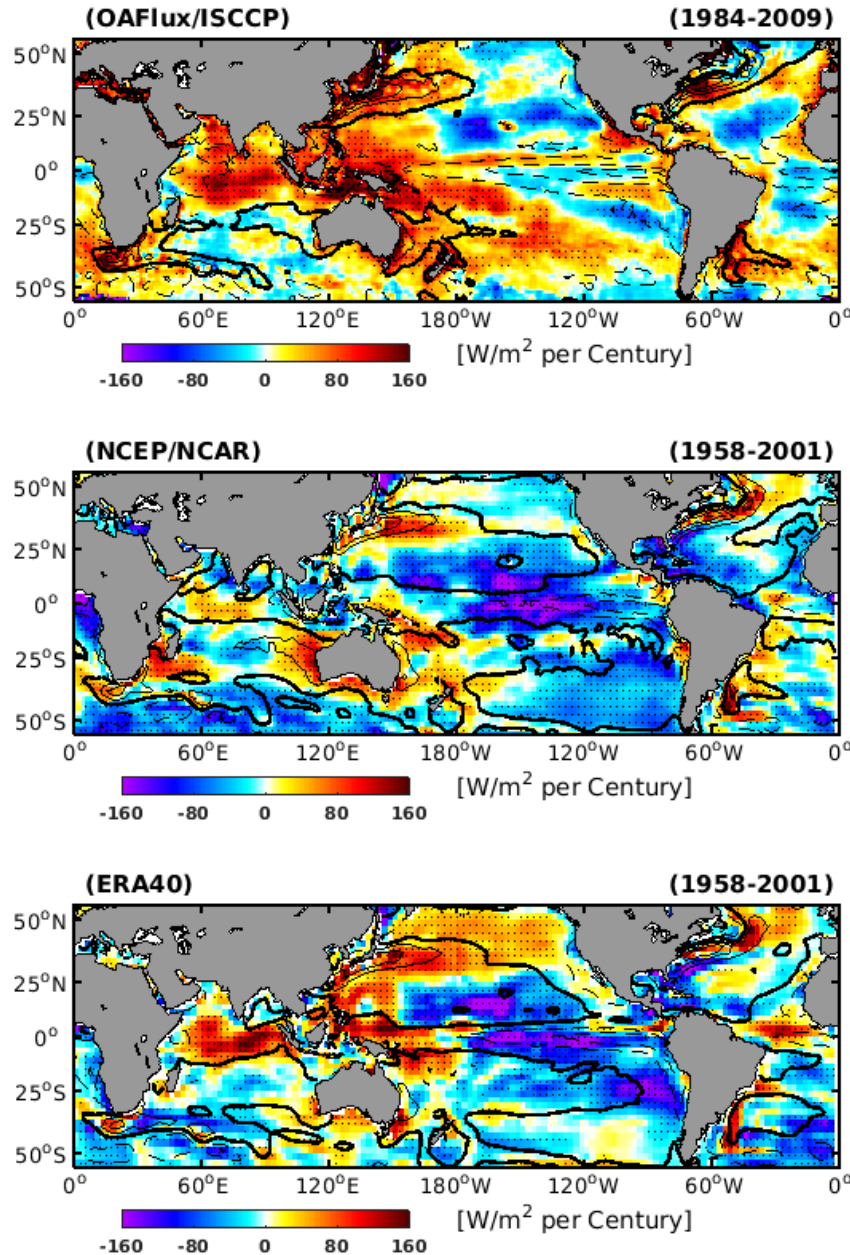
191 as illustrated by both reanalysis data sets, indicating an equatorward displacement of the Kuroshio
 192 Current over the period 1958–2001.

193 Comparing with the reanalysis data sets, the satellite-blended data sets also show stronger
 194 increases in Q_{net} and SST over the polar flank of the Agulhas Current (Figs. 3 and 4). While,
 195 due to their relatively short temporal period, the satellite-blended data sets are not able to iden-
 196 tify signals of asymmetrical increases in the two elements over the other four WBCs.

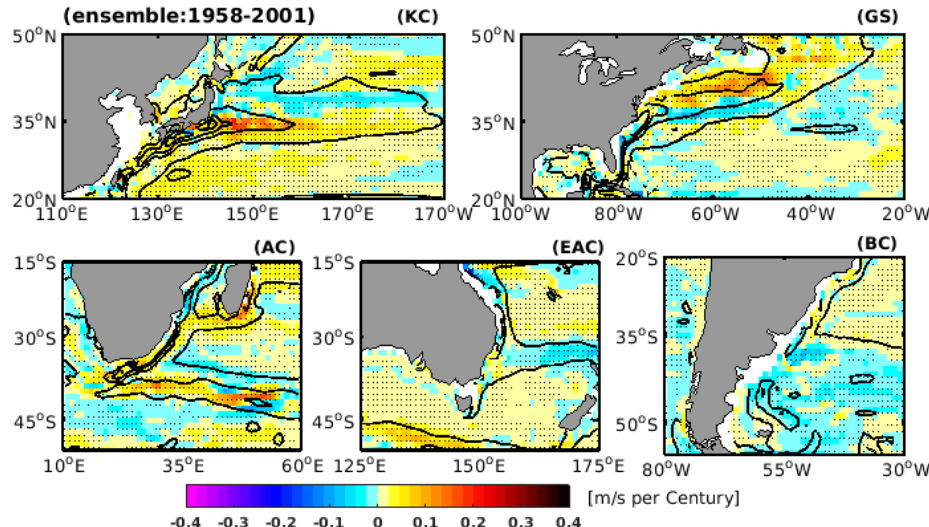
200 In order to cross validate our results found from the ocean surface, we analyze the ocean
 201 velocity field. The imprint of the global warming on the ocean water velocity from four ocean
 202 reanalysis data sets is presented in the Supplementary Figs. S1, S2, S3, S4. Since the WBCs
 203 are strong ocean currents, the background ocean velocity field (contour lines) indicates the cli-
 204 matological paths. The shading gives the changes in velocity speed. These ocean reanalyses
 205 show large discrepancies in terms of regional patterns of WBCs changes. Even the same model
 206 system (GECCO and GECCO2) does not produce consistent results, mostly likely, due to high
 207 nonlinearity of the WBCs and insufficient number of ocean observations assimilated in the ocean
 208 reanalysis data sets. We show the ensemble mean change of upper ocean water velocity in Fig. 5.
 209 Over the North Atlantic Ocean, a faster (slower) velocity over the polar (equator) flank of the
 210 Gulf Stream is observed, demonstrating a significant poleward shift of the Gulf Stream route.
 211 Over the south-western Indian Ocean, there is a prominent positive trend of the Agulhas Cur-
 212 rent along the continental shelf of south-eastern Africa. In contrast, a reduced velocity is found
 213 at the route of the Agulhas Current in the Mozambique Channel, demonstrating that the Ag-
 214 ulhas Current is stronger and shifting southwards. For the Eastern Australian Current and the
 215 Brazil Current, the ensemble members (see Supplementary Fig. S1, S2, S3, S4) show large
 216 differences, which makes the ensemble mean meaningless. Nevertheless, the SODA data set
 217 shows an intensified and southward shift of both the Brazil Current and the Eastern Australian
 218 Current.



178 **Figure 3.** Observational trends in SST (shading). Black contours present climatological SST. Stippling
179 indicates regions where the trends pass the 95% confidence level (Student's *t*-test).



180 **Figure 4.** Observational trends in Q_{net} (shading, positive-upward). Black contours present climatological
 181 Q_{net} . Upward Q_{net} is in solid lines; downward Q_{net} is in dashed lines; zero Q_{net} is in bold lines. Stippling
 182 indicates regions where the trends pass the 95% confidence level (Student's t -test).



197 **Figure 5.** Ensemble trends in upper 100 m ocean velocity (shading) based on SODA, ORA-S4, GECCO
 198 and GECCO2 ocean reanalyses. Contours: climatological depth-averaged (upper 100 m) sea water velocity.
 199 Stippling indicates areas where at least 3 data sets agree on the sign of the trends.

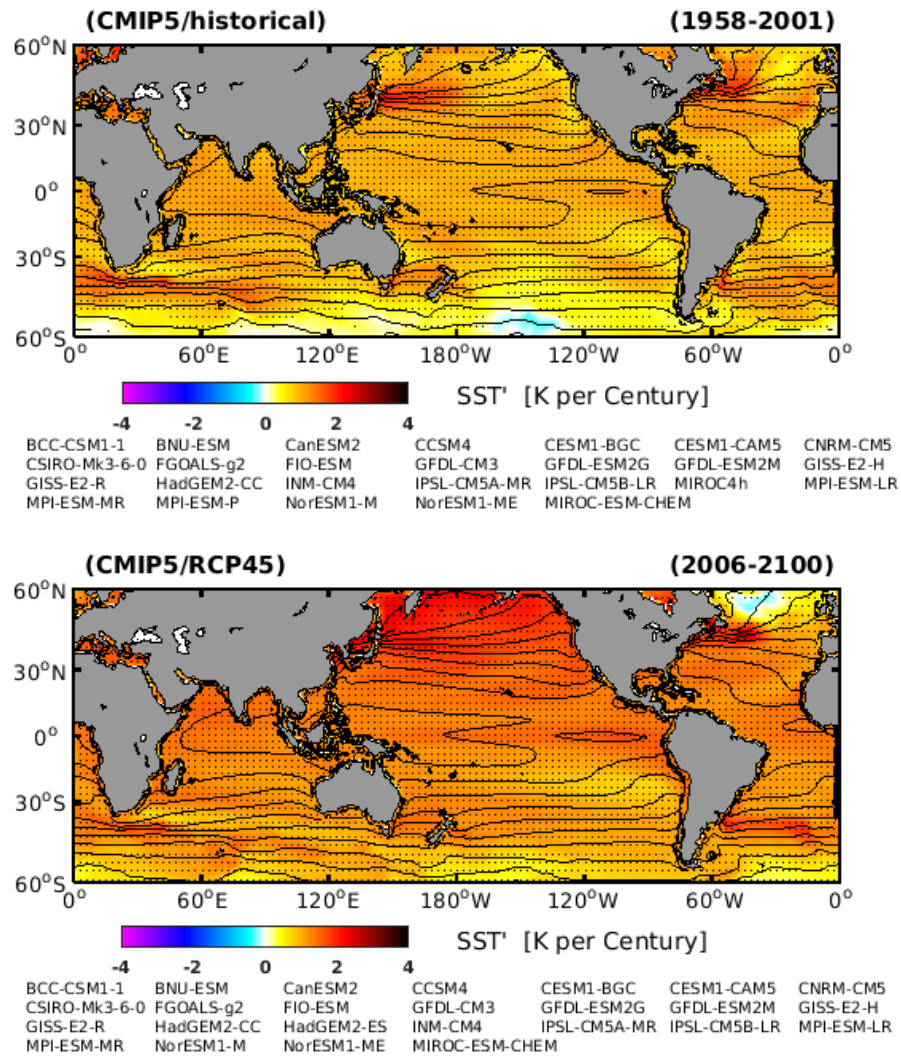
219 Over the North Pacific Ocean, we find that the Kuroshio Current is stronger and shifting
 220 towards the equator, which is again different from the other four WBCs. However, the re-
 221 sults in the velocity field are in agreement with the observational Q_{net} trends presented in the
 222 previous section (e.g., Fig. 4).

223 3.2 Results from climate models

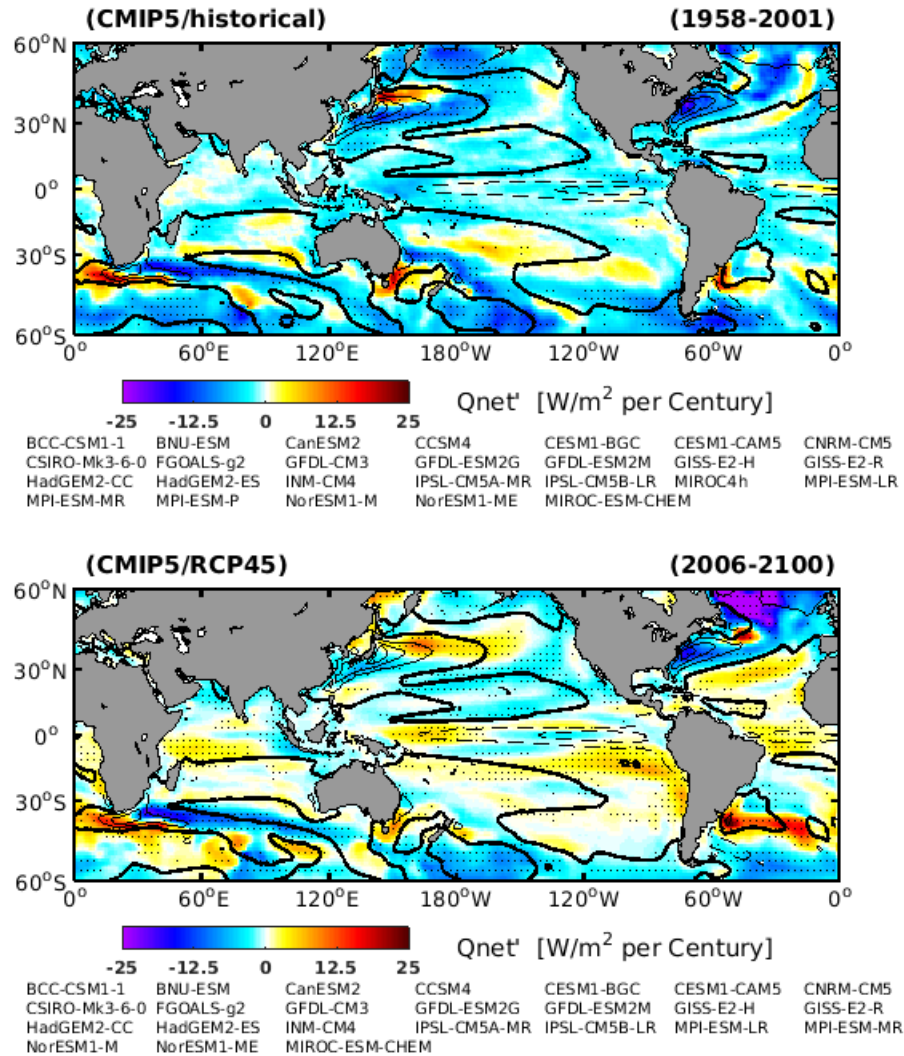
224 In this section, the dynamic changes of the WBCs are assessed on the basis of *historical*
 225 and *RCP4.5* simulations from CMIP5 archives (Figs. 6, 7, 8 and Fig. 9, respectively). In
 226 order to suppress the internal fluctuations, we analyze the ensemble mean of 27 climate mod-
 227 els. In general, the climate models present very similar patterns of WBCs climate changes over
 228 the Southern Hemisphere in comparison with observations. Over the Agulhas Current, the East
 229 Australian Current and the Brazil Current, the location of the maximum SST increase is found
 230 over the polar flanks of their mid-latitude expansions. Meanwhile, a relatively weak SST in-
 231 crease is found over their equatorial flanks. The corresponding Q_{net} trend exhibits dipole modes
 232 (positive values at the polar flank and negative values at the equator flank) over their mid-latitude
 233 expansions. Also, the ocean velocity trends over the above WBCs consistently illustrate in-
 234 creasing and poleward shifting of these currents.

235 Due to the large internal variability of the Northern Hemisphere WBCs (Fig. 2), there
 236 are strong discrepancies between the observations and climate models, e.g. the strengthen-
 237 & poleward shift of the Kuroshio Current and a significant weakening Gulf Stream, with re-
 238 ducing Q_{net} and decreasing ocean velocity (Figs. 6, 7, 8 and Fig. 9).

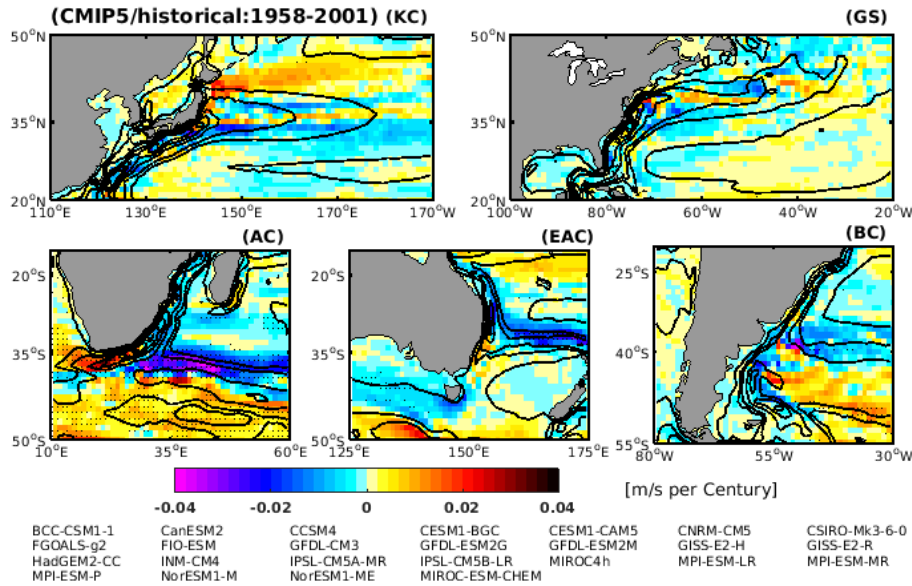
239 We notice that the ensemble results in the *historical* simulations are less pronounced
 240 compared to the *RCP4.5* simulations, because the global warming signal in the *historical*
 241 simulations is not beyond the model internal variability.



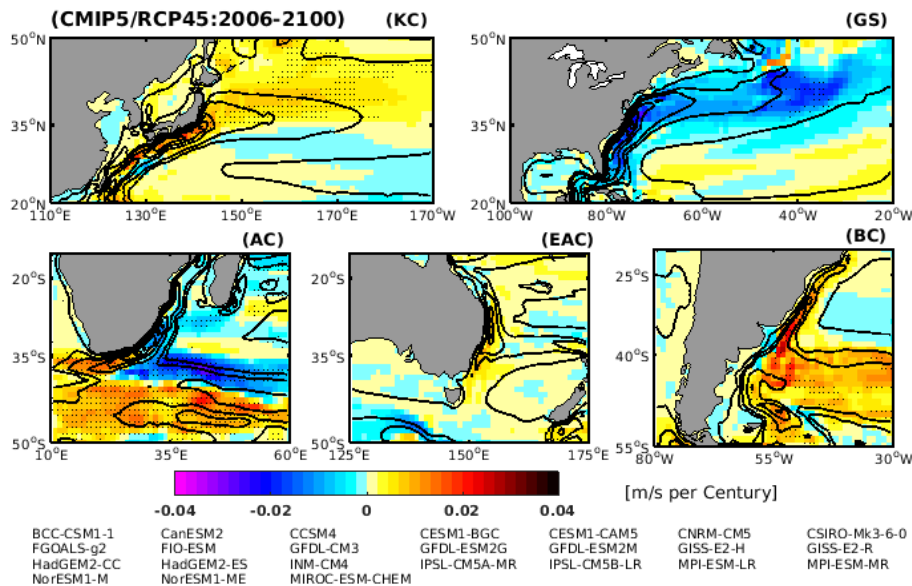
235 **Figure 6.** As in Fig. 3, but for ensemble trends based on the *historical* and *RCP4.5* simulations. Stippling
236 indicates areas where at least 2/3 of the models agree on the sign of the change.



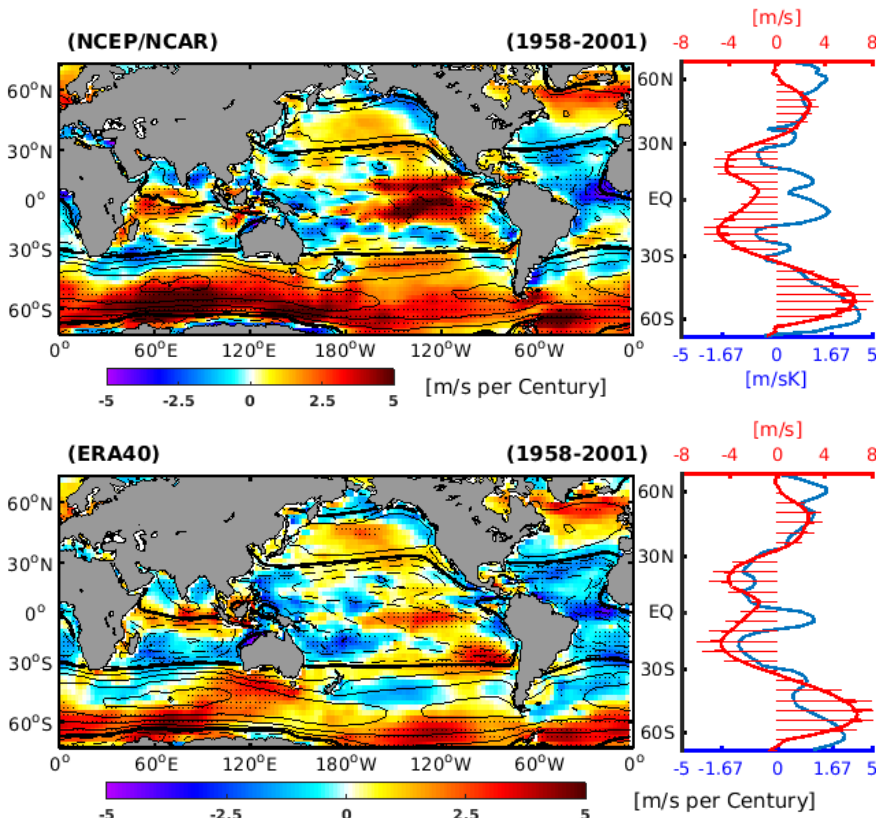
237 **Figure 7.** As in Fig. 4, but for ensemble trends based on the *historical* and *RCP4.5* simulations. Stip-
238 pling indicates areas where at least 2/3 of the models agree on the sign of the change.



243 **Figure 8.** As in Fig. 5, but for multi-model ensemble trends in ocean water velocity from the *historical*
244 simulations.



245 **Figure 9.** As in Fig. 8, but for multi-model ensemble trends in ocean water velocity from the *RCP4.5*
246 simulations.



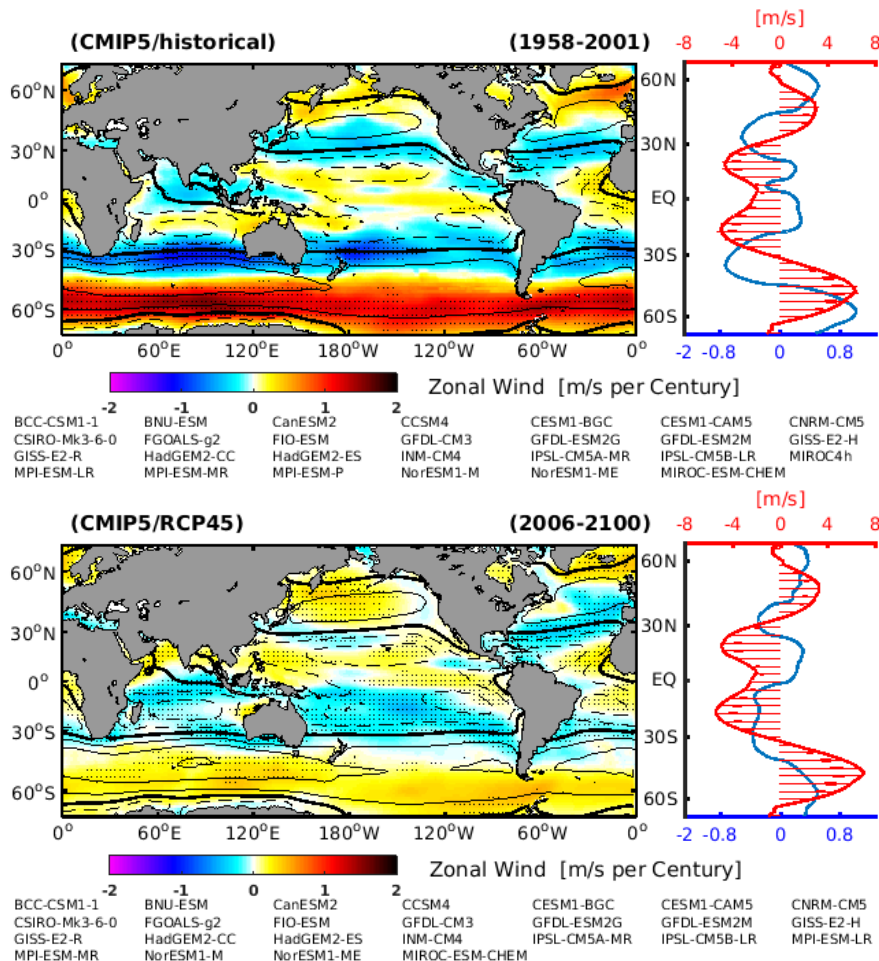
255 **Figure 10.** Left: trends (shaded) and climatology (contours) near-surface ocean zonal wind. Easterly winds
 256 are in solid lines; westerly winds are in dashed lines; zero zonal winds are bold. Right: Zonally averaged
 257 trend (blue) and climatology (red with arrow) of near-surface ocean zonal winds.

250 4 Possible mechanism

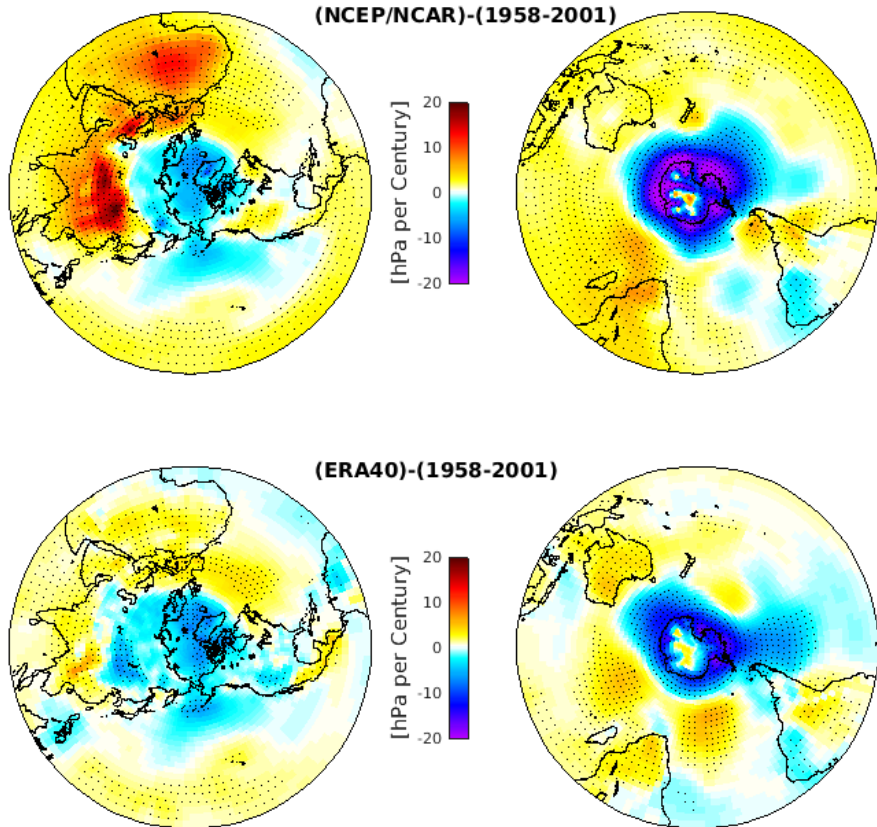
251 The easterly winds over low latitudes, associated with the westerly winds over high latitudes,
 252 largely drive the anti-cyclonic subtropical ocean gyres, which show an intensification
 253 over the western boundary (Fig. 1) [Pedlosky, 1996]. Significant dynamic changes of WBCs
 254 hint that the near-surface ocean zonal wind may have changed.

255 Figs. 10 and 11 show the trends of the near-surface ocean zonal winds in the observational
 256 data sets and CMIP5 simulations, respectively. Over the Southern Hemisphere, the wind
 257 trends over the mid and high latitudes are dominated by stronger westerly winds. Meanwhile,
 258 stronger easterly winds are found over most of the subtropical regions. Such trends reinforce
 259 the background zonal winds. As a consequence, the wind shear between the low and the high
 260 latitudes (wind stress curl) becomes stronger, which can force stronger WBCs in a warming
 261 climate. Besides the intensification of the zonal wind, all data sets consistently show that the
 262 zonal mean winds are shifting towards the South Pole in comparison with their climatology
 263 profile (Figs. 10 and 11, right-side). Such shifts show dynamic consistency with the poleward
 264 shift of the Southern Hemisphere WBCs.

265 Over the North Atlantic, all the data sets consistently show a stronger and poleward shift
 266 of zonal wind. However, over North Pacific, some discrepancies appear between the obser-
 267 vations (1958-2001) and climate models. Both atmospheric reanalyses present a stronger and
 268 equatorward shift of the North Pacific westerlies during 1958-2001, which contribute to a stronger
 269 and equatorward shift of the Kuroshio Current, (section 3.1). In contrast, the CMIP5 models



258 **Figure 11.** As in Fig. 10, but for multi-model ensemble trends in near-surface ocean zonal winds from the
 259 *historical* and *RCP4.5* simulations.

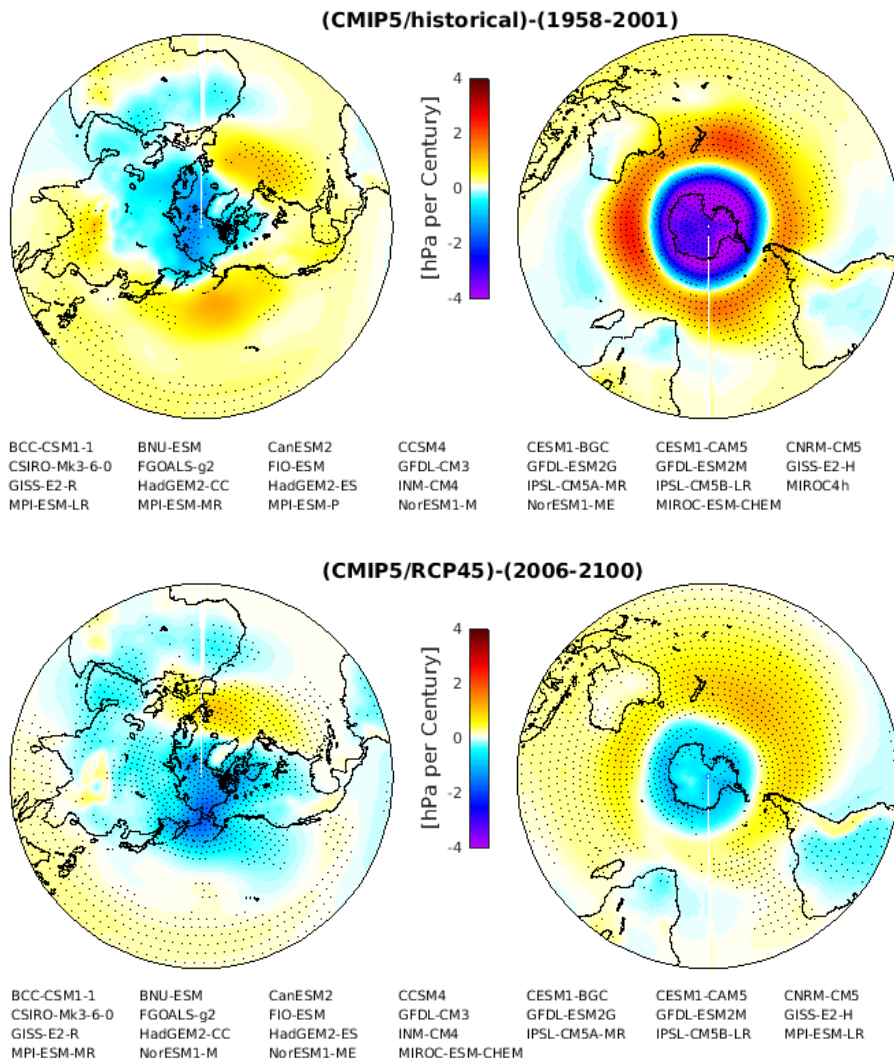


282 **Figure 12.** Trends in SLP based on the NCEP/NCAR and ERA40 data sets, respectively.

283
284
285
286
287
288
289
simulate stronger and poleward shift of the North Pacific westerlies, forcing a stronger and poleward shift of the Kuroshio Current, as identified in Section 3.2. To explore the reason for the differences over Northern Pacific, we present the long-term (1900-2010) trends of surface wind based on the century long reanalyses (Supplementary Figs. S5). Both 20CRv2 and ERA-20C consistently presents a stronger and poleward shift of the Northern Pacific westerly, indicating the observed equatorward shift during 1958-2001 are attribute to internal variability, as also shown in Fig. 2.

290
291
292
293
294
295
296
297
Associated with the near-surface wind, the SLP trends are displayed in Figs. 12 and 13, respectively. Both the observations as well as the CMIP5 models consistently show a decreasing SLP over the Poles and increasing SLP over mid latitudes of both Hemispheres. It is worth noting that the results based on the 20CRv2 and ERA-20C (Supplementary Figs. S6) resemble the patterns as we have identified here.

298
299
300
301
302
303
The near-surface ocean zonal wind and SLP show similar features as the positive phase of the annular modes (Northern Annular Mode (NAM) and Southern Annular Mode (SAM)), which are characterized by stronger and poleward shifts of the westerly winds, associated with negative SLP anomalies over high latitudes and positive SLP anomalies over mid latitudes. We propose that the positive annular mode-like trends contribute to the intensification of the near-surface ocean zonal winds and to shift them poleward. The changing winds force a strengthening and poleward displacement of the WBCs. As a result, more heat is transported from the tropics to the mid and high latitudes, which could significantly increase the SST and ocean



283 **Figure 13.** As in Fig. 12, but for the multi-model ensemble trends in SLP based on the *historical* and
 284 *RCP4.5* simulations.

heat loss (Q_{net}) there. Moreover, as the routes of the WBCs are shifting poleward, the position of the high Q_{net} over the WBCs will also shift poleward.

5 Discussion

Wu et al. [2012] investigated the WBCs dynamic changes based on two century-long reanalyses data sets, the 20CRv2 and the Simple Ocean Data Assimilation (SODA) [*Giese and Ray*, 2011]. However, the detection of the WBCs dynamics changes is challenging due to limited observations and the uncertainties in the data sets [*Wu et al.*, 2012; *Stocker et al.*, 2013]. To further explore this, we use more independent data sets and more metrics to identify and explain the dynamic changes of WBCs. The common features among these broad ranges of data resources indicate that the WBCs (except the Gulf Stream) are strengthening and shifting towards the poles in a warming climate.

Over the Southern Hemisphere, observational data and climate models show consistent results. However, over the Northern Hemisphere, the observed Gulf Stream and Kuroshio Current have strong decadal variations, as shown in Fig. 2. Observations (climate models) record an equatorward (poleward) shift of the Kuroshio Current over the period 1958-2001. *Seager et al.* [2001]; *Taguchi et al.* [2007]; *Sasaki and Schneider* [2011] demonstrated that the 1976/77 equatorward shift in basin-scale winds contributed to the corresponding movement of the Kuroshio Current. However, from a long term perspective (1900-2010), both 20CRv2 and ERA-20C present a poleward shift of surface wind over the Pacific Ocean (supplementary Figs. S5), indicating the observed equatorward shift of Kuroshio Current over the period 1958-2001 is likely to be due to natural climate variations. Over the North Atlantic Ocean, the observations during 1958-2001 present a stronger and poleward shift of the Gulf Stream (consistent with the surface wind), while the climate models show a weakening of the Gulf Stream in response to global warming. The Gulf Stream is part of the upper branch of the Atlantic Meridional Overturning Circulation (AMOC). Strength of the Gulf Stream is determined not only by the near-surface ocean wind, but also by the AMOC, particularly on multi-decadal and centennial time scales. The simulated weakening of AMOC [e.g., *Lohmann et al.*, 2008; *Cheng et al.*, 2013] is linked to the weakening Gulf Stream.

Regarding the potential driving mechanism, several previous studies have focused on the climate change over individual WBCs. *Sakamoto et al.* [2005] have investigated the responses of the Kuroshio Current to global warming and suggested that a strengthening of the Kuroshio Current is caused by an El Niño-like mode. Indeed, the climate phenomenon over the Pacific Ocean (i.e., ENSO, PDO) plays a vital role in the variability of the Kuroshio Current, particularly on interannual to decadal time scales [*Qiu, 2003; Qiu and Chen, 2005; Taguchi et al., 2007; Andres et al., 2009; Sasaki and Schneider, 2011*]. However, we found that the common features of WBCs changes are characterized by an intensification and a poleward shift. Such changes are not an isolated phenomenon over individual ocean basins, but a global effect. Thus, the dynamic changes of the WBCs should be caused by a factor that can influence all ocean basins, such as we proposed, the positive annular mode-like trends over both hemispheres. Previously, the typical features of the annular modes in the wind field are described as an intensification and poleward shift of the westerly winds [*Thompson and Wallace, 2000*]. Here, we suggest that both the easterly winds over the low latitudes and the westerly winds over the mid and high latitudes have strengthened. Meanwhile, the profile of the zonal winds is shifting poleward over both hemispheres. The systematic changes in zonal winds are consistent with the poleward shift of the Hadley Cell [*Hu and Fu, 2007; Lu et al., 2007; Johanson and Fu, 2009*], the expansion of the tropical belt [*Santer et al., 2003; Seidel and Randel, 2007; Seidel et al., 2007; Fu and Lin, 2011*], and the poleward shift of the subtropical dry zones [*Previdi and Liepert, 2007*].

Sato et al. [2006] demonstrated that the Arctic Oscillation-like trends are responses to a northward shift of the subtropical wind-driven gyre in the North Pacific Ocean. *Curry and McCartney* [2001] proved that the transport of the Gulf Stream has intensified due to a stronger

349 North Atlantic Oscillation after the 1960s. Their conclusions are in agreement with ours, be-
 350 cause the North Atlantic Oscillation and the Arctic Oscillation (or NAM) show very similar
 351 evolutions [Deser, 2000; Rogers and McHugh, 2002; Feldstein and Franzke, 2006]. Observa-
 352 tions show a stronger NAM during the past several decades. However, a weaker NAM from
 353 the late 1990s is observed [Thompson and Wallace, 2000] simultaneously with the global warm-
 354 ing hiatus [Easterling and Wehner, 2009]. Several factors are suggested having impact on the
 355 variations of NAM, i.e., the greenhouse gases, the stratosphere-troposphere interaction, local
 356 sea ice variability and remote tropical influence [Fyfe et al., 1999; Wang and Chen, 2010; Gillett
 357 and Fyfe, 2013; Cattiaux and Cassou, 2013]. The trend in Northern Annular Mode during 1958-
 358 2001 is most likely dominated by its natural variations. However, for a longer time period, both
 359 the century-long atmosphere reanalyses (i.e., 20CRv2 and ERA-20C in supplementary Figs.
 360 S5, S6) and the CMIP5 climate models illustrate that the NAM is propagating to a positive
 361 phase under global warming.

362 Over the Southern Hemisphere, several studies have also confirmed that the Southern
 363 Hemisphere subtropical gyres are influenced by the SAM [Hall and Visbeck, 2002; Cai et al.,
 364 2005; Sen Gupta and England, 2006; Cai, 2006; Fyfe and Saenko, 2006; Sen Gupta et al., 2009].
 365 Both observations [Thompson and Wallace, 2000; Marshall, 2003] and CGCM simulations [Fyfe
 366 et al., 1999; Stone et al., 2001; Kushner et al., 2001; Cai et al., 2003; Gillett and Thompson,
 367 2003; Rauthe et al., 2004; Arblaster and Meehl, 2006; Gillett and Fyfe, 2013] show that the
 368 SAM is entering a positive phase. The ozone depletion was suggested to be the main driver
 369 for the observed positive trend of SAM [Thompson and Solomon, 2002; Kindem and Chris-
 370 tiansen, 2001; Sexton, 2001; Gillett and Thompson, 2003; Thompson et al., 2011; Polvani et al.,
 371 2011]. However, increasing greenhouse gases were also suggested to have a contribution on
 372 it [Fyfe et al., 1999; Kushner et al., 2001; Cai et al., 2003; Rauthe et al., 2004]. As it is shown
 373 in Fig. 11 and 13, a stronger SAM trend is found during 1958-2001 when both the ozone de-
 374 pletion and the increasing greenhouse gas force the SAM. However, in the near future, as ozone
 375 levels recover, it will play an opposite role as increasing greenhouse gas. The positive trend in
 376 SAM might be weaker or reverse sign over the coming decades [Arblaster et al., 2011].

377 WBCs have a broad impact on the climate and economy over the adjacent mainland, e.g.,
 378 the temperature, fishing, storms, precipitation and extreme climate events [Seager et al., 2002;
 379 Cai et al., 2005; Minobe et al., 2008]. As expected, stronger WBCs will increase the atmospheric
 380 baroclinicity, favoring more storms [Shaman et al., 2010]. Moreover, the adjacent regions of
 381 the WBCs suffer more warming than other regions, due to the increased heat transport by the
 382 WBCs, especially over Eastern Asian, where the Kuroshio Current transports much more heat
 383 [Tang et al., 2009]. In contrast, a weakening of the Gulf Stream in this century can reduce the
 384 heat release from the ocean, and contribute to a relative cooling over Europe and Eastern Amer-
 385 ica, a feature suggested by Dima and Lohmann [2010] and Rahmstorf et al. [2015]. We sug-
 386 gest that particular attention must be paid to the climate change over the adjacent regions of
 387 WBCs.

388 6 Conclusions

389 We find observational and model support for an intensification and poleward movement
 390 of WBCs in response to anthropogenic climate change. The one exception to this is the Gulf
 391 Stream where a weakening of the AMOC tends to reduce the strength of the Gulf Stream. Else-
 392 where the poleward shift is postulated to be driven by a poleward shift of the extratropical west-
 393 erlies and expansion of the Hadley Cell. In the Southern Hemisphere the observed record in-
 394 dicates this intensification and southward shift is already occurring perhaps because ozone de-
 395 pletion and rising greenhouse gas have worked in the same direction in forcing a positive SAM.
 396 In the Northern Hemisphere natural variability appears to be temporarily interrupting the pole-
 397 ward shift of the Kuroshio and have driven a poleward shift of the Gulf Stream via the up-
 398 ward trend in the Arctic Oscillation over the analyzed period (1958-2001). As the 21st cen-
 399 tury progresses, we expect the poleward shift in the Northern Hemisphere to become clearer
 400 as the response to radiative forcing grows in size relative to the natural variability. In the South-

ern Hemisphere changes in intensity and latitude of the WBCs will depend on the opposing impacts of ozone recovery, rising greenhouse gas and the varying influence of natural variability. In all cases, the dynamic changes of the WBCs impact poleward ocean heat transport, regional climate, storm tracks and ocean ecosystems. So, improved understanding and projection of how they will evolve is an important area of research to which the current work hopefully provides a useful impetus.

407 Acknowledgments

The first author acknowledges the helpful discussions with Xun Gong and Xu Zhang. We acknowledge the World Climate Research Programme's Working Group on Coupled Modelling, which is responsible for CMIP5, and we thank the climate modeling groups (listed in Table 2 of this paper) for producing and making available their model output. For CMIP the U.S. Department of Energy's Program for Climate Model Diagnosis and Intercomparison provides coordinating support and led development of software infrastructure in partnership with the Global Organization for Earth System Science Portals. We would like to express our gratitude and appreciation to the groups who freely distribute the data sets used in this work. These data sets can be accessed with the following links: HadISST (<http://www.metoffice.gov.uk/hadobs/hadisst/data/download.html>), HadCRUT4 (<http://www.metoffice.gov.uk/hadobs/hadcrut4/data/current/download.html>), OISST (<https://www.ncdc.noaa.gov/oisst/data-access>), OAFlux/ISCCP (ftp://ftp.whoi.edu/pub/science/oaflux/data_v3/monthly/), NCEP (ftp://ftp.cdc.noaa.gov/Datasets/ncep.reanalysis.derived/surface_gauss/), ERA40 and ERA-20C (<http://apps.ecmwf.int/datasets/>), 20CRv2 (http://www.esrl.noaa.gov/psd/data/gridded/data.20thC_ReanV2.monolevel.mm.html), ORA-S4 and GECCO/GECCO2 (<ftp://ftp.icdc.zmaw.de/EASYInit/>), SODA2.2.0 (http://dsrs.atmos.umd.edu/DATA/soda_2.2.0/SODA_2.2.0_), CMIP5 (<http://cera-www.dkrz.de/WDCC/ui/Index.jsp>). Finally, we thank the editor and two reviewers for their constructive comments, which helped us to improve the manuscript.

426 References

- 427 Andres, M., J.-H. Park, M. Wimbush, X.-H. Zhu, H. Nakamura, K. Kim, and K.-I. Chang
 428 (2009), Manifestation of the Pacific decadal oscillation in the Kuroshio, *Geophysical*
 429 *Research Letters*, 36(16).
- 430 Arblaster, J., G. Meehl, and D. Karoly (2011), Future climate change in the southern
 431 hemisphere: Competing effects of ozone and greenhouse gases, *Geophysical Research*
 432 *Letters*, 38(2).
- 433 Arblaster, J. M., and G. A. Meehl (2006), Contributions of external forcings to southern
 434 annular mode trends, *Journal of Climate*, 19(12), 2896–2905.
- 435 Balmaseda, M. A., K. Mogensen, and A. T. Weaver (2013), Evaluation of the ECMWF
 436 ocean reanalysis system ORAS4, *Quarterly Journal of the Royal Meteorological Society*,
 437 139(674), 1132–1161.
- 438 Bellucci, A., et al. (2014), An assessment of a multi-model ensemble of decadal climate
 439 predictions, *Climate Dynamics*, 44(9–10), 2787–2806.
- 440 Biastoch, A., C. W. Böning, F. U. Schwarzkopf, and J. Lutjeharms (2009), Increase in
 441 Agulhas leakage due to poleward shift of Southern Hemisphere westerlies, *Nature*,
 442 462(7272), 495–498.
- 443 Brunke, M. A., X. Zeng, and S. Anderson (2002), Uncertainties in sea surface turbulent
 444 flux algorithms and data sets, *Journal of Geophysical Research: Oceans* (1978–2012),
 445 107(C10), 5–1.
- 446 Cai, W. (2006), Antarctic ozone depletion causes an intensification of the Southern Ocean
 447 super-gyre circulation, *Geophysical Research Letters*, 33(3), L03,712.
- 448 Cai, W., P. H. Whetton, and D. J. Karoly (2003), The response of the Antarctic Oscillation
 449 to increasing and stabilized atmospheric CO₂, *Journal of Climate*, 16(10), 1525–1538.
- 450 Cai, W., G. Shi, T. Cowan, D. Bi, and J. Ribbe (2005), The response of the Southern An-
 451 nular Mode, the East Australian Current, and the southern mid-latitude ocean circulation

- 452 to global warming, *Geophysical Research Letters*, 32(23), L23,706.
- 453 Carton, J. A., and B. S. Giese (2008), A reanalysis of ocean climate using Simple Ocean
454 Data Assimilation (SODA), *Monthly Weather Review*, 136(8), 2999–3017.
- 455 Cattiaux, J., and C. Cassou (2013), Opposite CMIP3/CMIP5 trends in the wintertime
456 Northern Annular Mode explained by combined local sea ice and remote tropical influences,
457 *Geophysical Research Letters*, 40(14), 3682–3687.
- 458 Cheng, W., J. C. Chiang, and D. Zhang (2013), Atlantic Meridional Overturning Circula-
459 tion (AMOC) in CMIP5 Models: RCP and Historical Simulations, *Journal of Climate*,
460 26(18).
- 461 Colling, A. (2001), *Ocean circulation*, vol. 3, Butterworth-Heinemann.
- 462 Compo, G. P., J. S. Whitaker, and P. D. Sardeshmukh (2006), Feasibility of a 100-year
463 reanalysis using only surface pressure data, *Bulletin of the American Meteorological
464 Society*, 87(2), 175.
- 465 Compo, G. P., et al. (2011), The twentieth century reanalysis project, *Quarterly Journal of
466 the Royal Meteorological Society*, 137(654), 1–28.
- 467 Cronin, M. F., et al. (2010), Monitoring ocean-atmosphere interactions in western bound-
468 ary current extensions, in *Proceedings of the "OceanObs2010 09: Sustained Ocean
469 Observations and Information for Society" Conference*, vol. 2.
- 470 Curry, R. G., and M. S. McCartney (2001), Ocean gyre circulation changes associated
471 with the North Atlantic Oscillation, *Journal of Physical Oceanography*, 31(12), 3374–
472 3400.
- 473 Dee, D., M. Balmaseda, G. Balsamo, R. Engelen, A. Simmons, and J.-N. Thépaut (2014),
474 Toward a consistent reanalysis of the climate system, *Bulletin of the American Meteoro-
475 logical Society*, 95(8), 1235–1248.
- 476 Deser, C. (2000), On the teleconnectivity of the "Arctic Oscillation", *Geophysical Re-
477 search Letters*, 27(6), 779–782.
- 478 Deser, C., M. Alexander, and M. Timlin (1999), Evidence for a wind-driven intensification
479 of the Kuroshio Current Extension from the 1970s to the 1980s, *Journal of Climate*,
480 12(6), 1697–1706.
- 481 Dima, M., and G. Lohmann (2010), Evidence for two distinct modes of large-scale ocean
482 circulation changes over the last century, *Journal of Climate*, 23(1), 5–16.
- 483 Easterling, D. R., and M. F. Wehner (2009), Is the climate warming or cooling?, *Geophys-
484 ical Research Letters*, 36(8).
- 485 Feldstein, S. B., and C. Franzke (2006), Are the North Atlantic Oscillation and the north-
486 ern annular mode distinguishable?, *Journal of the Atmospheric Sciences*, 63(11), 2915–
487 2930.
- 488 Fu, Q., and P. Lin (2011), Poleward shift of subtropical jets inferred from satellite-
489 observed lower-stratospheric temperatures, *Journal of Climate*, 24(21), 5597–5603.
- 490 Fyfe, J., G. Boer, and G. Flato (1999), The Arctic and Antarctic Oscillations and their
491 projected changes under global warming, *Geophysical Research Letters*, 26(11), 1601–
492 1604.
- 493 Fyfe, J. C., and O. A. Saenko (2006), Simulated changes in the extratropical Southern
494 Hemisphere winds and currents, *Geophysical Research Letters*, 33(6).
- 495 Giese, B. S., and S. Ray (2011), El Niño variability in simple ocean data assimilation
496 (SODA), 1871–2008, *Journal of Geophysical Research: Oceans (1978–2012)*, 116(C2).
- 497 Gillett, N., and J. Fyfe (2013), Annular mode changes in the CMIP5 simulations, *Geo-
498 physical Research Letters*, 40(6), 1189–1193.
- 499 Gillett, N. P., and D. W. Thompson (2003), Simulation of recent Southern Hemisphere
500 climate change, *Science*, 302(5643), 273–275.
- 501 Goni, G. J., F. Bringas, and P. N. DiNezio (2011), Observed low frequency variability
502 of the Brazil Current front, *Journal of Geophysical Research: Oceans (1978–2012)*,
503 116(C10).
- 504 Gulev, S., T. Jung, and E. Ruprecht (2007), Estimation of the impact of sampling errors in
505 the VOS observations on air-sea fluxes. Part I: Uncertainties in climate means, *Journal*

- 506 *of Climate*, 20(2), 279–301.
- 507 Hall, A., and M. Visbeck (2002), Synchronous Variability in the Southern Hemisphere
508 Atmosphere, Sea Ice, and Ocean Resulting from the Annular Mode, *Journal of Climate*,
509 15(21), 3043–3057.
- 510 Hu, Y., and Q. Fu (2007), Observed poleward expansion of the Hadley circulation since
511 1979, *Atmospheric Chemistry and Physics*, 7(19), 5229–5236.
- 512 Inatsu, M., H. Mukougawa, and S. Xie (2002), Tropical and extratropical SST effects
513 on the midlatitude storm track, *Journal of the Meteorological Society of Japan*, 80(4B),
514 1069–1076.
- 515 Johanson, C. M., and Q. Fu (2009), Hadley cell widening: Model simulations versus
516 observations, *Journal of Climate*, 22(10), 2713–2725.
- 517 Kalnay, E., et al. (1996), The NCEP/NCAR 40-year reanalysis project, *Bulletin of the*
518 *American Meteorological Society*, 77(3), 437–471.
- 519 Kelly, K. A., M. J. Caruso, S. Singh, and B. Qiu (1996), Observations of atmosphere-
520 ocean coupling in midlatitude western boundary currents, *Journal of Geophysical Re-*
521 *search: Oceans (1978–2012)*, 101(C3), 6295–6312.
- 522 Kindem, I. T., and B. Christiansen (2001), Tropospheric response to stratospheric ozone
523 loss, *Geophysical Research Letters*, 28(8), 1547–1550.
- 524 Köhl, A. (2015), Evaluation of the GECCO2 ocean synthesis: transports of volume, heat
525 and freshwater in the Atlantic, *Quarterly Journal of the Royal Meteorological Society*,
526 141(686), 166–181.
- 527 Köhl, A., and D. Stammer (2008), Variability of the meridional overturning in the North
528 Atlantic from the 50-year GECCO state estimation, *Journal of Physical Oceanography*,
529 38(9), 1913–1930.
- 530 Krueger, O., F. Schenk, F. Feser, and R. Weisse (2013), Inconsistencies between long-
531 term trends in storminess derived from the 20cr reanalysis and observations, *Journal of*
532 *Climate*, 26(3), 868–874.
- 533 Kushner, P. J., I. M. Held, and T. L. Delworth (2001), Southern Hemisphere atmospheric
534 circulation response to global warming, *Journal of Climate*, 14(10), 2238–2249.
- 535 L'Ecuyer, T. S., and G. L. Stephens (2003), The tropical oceanic energy budget from the
536 TRMM perspective. Part I: Algorithm and uncertainties, *Journal of climate*, 16(12),
537 1967–1985.
- 538 Lohmann, G., H. Haak, and J. H. Jungclaus (2008), Estimating trends of Atlantic merid-
539 ional overturning circulation from long-term hydrographic data and model simulations,
540 *Ocean Dynamics*, 58(2), 127–138.
- 541 Lu, J., G. A. Vecchi, and T. Reichler (2007), Expansion of the Hadley cell under global
542 warming, *Geophysical Research Letters*, 34(6).
- 543 Mantua, N. J., S. R. Hare, Y. Zhang, J. M. Wallace, and R. C. Francis (1997), A Pacific
544 interdecadal climate oscillation with impacts on salmon production, *Bulletin of the*
545 *American Meteorological Society*, 78(6), 1069–1079.
- 546 Marshall, G. J. (2003), Trends in the Southern Annular Mode from observations and
547 reanalyses, *Journal of Climate*, 16(24), 4134–4143.
- 548 Meehl, G. A., C. Covey, K. E. Taylor, T. Delworth, R. J. Stouffer, M. Latif, B. McAvaney,
549 and J. F. Mitchell (2007), The WCRP CMIP3 multimodel dataset: A new era in climate
550 change research, *Bulletin of the American Meteorological Society*, 88(9), 1383–1394.
- 551 Minobe, S., A. Kuwano-Yoshida, N. Komori, S. P. Xie, and R. J. Small (2008), Influence
552 of the Gulf Stream on the troposphere, *Nature*, 452(7184), 206–209.
- 553 Morice, C. P., J. J. Kennedy, N. A. Rayner, and P. D. Jones (2012), Quantifying uncer-
554 tainties in global and regional temperature change using an ensemble of observational
555 estimates: The HadCRUT4 data set, *Journal of Geophysical Research: Atmospheres*
556 (1984–2012), 117(D8).
- 557 Pedlosky, J. (1996), *Ocean circulation theory*, Springer Science & Business Media.
- 558 Poli, P., et al. (2016), Era-20c: An atmospheric reanalysis of the 20th century, *Journal of*
559 *Climate*, 0(2016).

- 560 Polvani, L. M., D. W. Waugh, G. J. Correa, and S.-W. Son (2011), Stratospheric ozone
 561 depletion: The main driver of twentieth-century atmospheric circulation changes in the
 562 southern hemisphere, *Journal of Climate*, 24(3), 795–812.
- 563 Previdi, M., and B. G. Liepert (2007), Annular modes and Hadley cell expansion under
 564 global warming, *Geophysical Research Letters*, 34(22).
- 565 Qiu, B. (2003), Kuroshio Extension variability and forcing of the Pacific decadal oscil-
 566 lations: Responses and potential feedback, *Journal of Physical Oceanography*, 33(12),
 567 2465–2482.
- 568 Qiu, B., and S. Chen (2005), Variability of the Kuroshio Extension jet, recirculation
 569 gyre, and mesoscale eddies on decadal time scales, *Journal of Physical Oceanography*,
 570 35(11), 2090–2103.
- 571 Qiu, B., and S. Chen (2006), Decadal variability in the large-scale sea surface height field
 572 of the South Pacific Ocean: Observations and causes, *Journal of Physical Oceanogra-*
 573 *phy*, 36(9), 1751–1762.
- 574 Rahmstorf, S., G. Feulner, M. E. Mann, A. Robinson, S. Rutherford, and E. J. Schaffer-
 575 nicht (2015), Exceptional twentieth-century slowdown in Atlantic Ocean overturning
 576 circulation, *Nature Climate Change*.
- 577 Rauthé, M., A. Hense, and H. Paeth (2004), A model intercomparison study of climate
 578 change-signals in extratropical circulation, *International Journal of Climatology*, 24(5),
 579 643–662.
- 580 Rayner, N., D. Parker, E. Horton, C. Folland, L. Alexander, D. Rowell, E. Kent, and
 581 A. Kaplan (2003), Global analyses of sea surface temperature, sea ice, and night ma-
 582 rine air temperature since the late nineteenth century, *Journal of Geophysical Research:*
Atmospheres (1984–2012), 108(D14).
- 584 Refsgaard, J. C., et al. (2014), A framework for testing the ability of models to project
 585 climate change and its impacts, *Climatic Change*, 122(1-2), 271–282.
- 586 Reynolds, R. W., N. A. Rayner, T. M. Smith, D. C. Stokes, and W. Wang (2002), An
 587 improved in situ and satellite SST analysis for climate, *Journal of Climate*, 15(13),
 588 1609–1625.
- 589 Ridgway, K. (2007), Long-term trend and decadal variability of the southward penetra-
 590 tion of the East Australian Current, *Geophysical Research Letters*, 34(13).
- 591 Ridgway, K., R. Coleman, R. Bailey, and P. Sutton (2008), Decadal variability of East
 592 Australian Current transport inferred from repeated high-density XBT transects, a CTD
 593 survey and satellite altimetry, *Journal of Geophysical Research: Oceans* (1978–2012),
 594 113(C8).
- 595 Roemmich, D., J. Gilson, R. Davis, P. Sutton, S. Wijffels, and S. Riser (2007), Decadal
 596 spinup of the South Pacific subtropical gyre, *Journal of Physical Oceanography*, 37(2),
 597 162–173.
- 598 Rogers, J., and M. McHugh (2002), On the separability of the North Atlantic Oscillation
 599 and Arctic Oscillation, *Climate Dynamics*, 19(7), 599–608.
- 600 Rossow, W. B., and R. A. Schiffer (1991), ISCCP cloud data products, *Bulletin of the*
American Meteorological Society, 72(1), 2–20.
- 602 Sakamoto, T. T., H. Hasumi, M. Ishii, S. Emori, T. Suzuki, T. Nishimura, and A. Sumi
 603 (2005), Responses of the Kuroshio and the Kuroshio Extension to global warming in a
 604 high-resolution climate model, *Geophysical Research Letters*, 32(14).
- 605 Santer, B. D., et al. (2003), Contributions of anthropogenic and natural forcing to recent
 606 tropopause height changes, *Science*, 301(5632), 479–483.
- 607 Sasaki, Y. N., and N. Schneider (2011), Decadal Shifts of the Kuroshio Extension Jet:
 608 Application of Thin-Jet Theory, *Journal of Physical Oceanography*, 41(5), 979–993.
- 609 Sato, Y., S. Yukimoto, H. Tsujino, H. Ishizaki, and A. Noda (2006), Response of North
 610 Pacific ocean circulation in a Kuroshio-resolving ocean model to an Arctic Oscillation
 611 (AO)-like change in Northern Hemisphere atmospheric circulation due to greenhouse-
 612 gas forcing, *Journal of the Meteorological Society of Japan*, 84(2), 295–309.

- Schlesinger, M. E., and N. Ramankutty (1994), An oscillation in the global climate system of period 65–70 years, *Nature*, 367(6465), 723–726.
- Seager, R., Y. Kushnir, N. H. Naik, M. A. Cane, and J. Miller (2001), Wind-Driven Shifts in the Latitude of the Kuroshio-Oyashio Extension and Generation of SST Anomalies on Decadal Timescales, *Journal of Climate*, 14(22), 4249–4265.
- Seager, R., D. S. Battisti, J. Yin, N. Gordon, N. Naik, A. C. Clement, and M. A. Cane (2002), Is the Gulf Stream responsible for Europe's mild winters?, *Quarterly Journal of the Royal Meteorological Society*, 128(586), 2563–2586.
- Seidel, D. J., and W. J. Randel (2007), Recent widening of the tropical belt: Evidence from tropopause observations, *Journal of Geophysical Research: Atmospheres* (1984–2012), 112(D20).
- Seidel, D. J., Q. Fu, W. J. Randel, and T. J. Reichler (2007), Widening of the tropical belt in a changing climate, *Nature Geoscience*, 1(1), 21–24.
- Sen Gupta, A., and M. H. England (2006), Coupled ocean-atmosphere-ice response to variations in the Southern Annular Mode, *Journal of Climate*, 19(18), 4457–4486.
- Sen Gupta, A., A. Santoso, A. S. Taschetto, C. C. Ummenhofer, J. Trevena, and M. H. England (2009), Projected changes to the Southern Hemisphere ocean and sea ice in the IPCC AR4 climate models, *Journal of Climate*, 22(11), 3047–3078.
- Sexton, D. (2001), The effect of stratospheric ozone depletion on the phase of the Antarctic Oscillation, *Geophysical Research Letters*, 28(19), 3697–3700.
- Shaman, J., R. Samelson, and E. Skyllingstad (2010), Air-sea fluxes over the Gulf Stream region: atmospheric controls and trends, *Journal of Climate*, 23(10), 2651–2670.
- Stocker, T. F., et al. (2013), Climate Change 2013. The Physical Science Basis. Working Group I Contribution to the Fifth Assessment Report of the Intergovernmental Panel on Climate Change-Abstract for decision-makers, *Tech. rep.*, Groupe d'experts intergouvernemental sur l'évolution du climat/Intergovernmental Panel on Climate Change-IPCC, C/O World Meteorological Organization, 7bis Avenue de la Paix, CP 2300 CH-1211 Geneva 2 (Switzerland).
- Stone, D., A. J. Weaver, and R. J. Stouffer (2001), Projection of climate change onto modes of atmospheric variability, *Journal of Climate*, 14(17), 3551–3565.
- Taguchi, B., S.-P. Xie, N. Schneider, M. Nonaka, H. Sasaki, and Y. Sasai (2007), Decadal Variability of the Kuroshio Extension: Observations and an Eddy-Resolving Model Hindcast, *Journal of Climate*, 20(11), 2357–2377.
- Taguchi, B., H. Nakamura, M. Nonaka, and S. Xie (2009), Influences of the Kuroshio/Oyashio Extensions on Air-Sea Heat Exchanges and Storm-Track Activity as Revealed in Regional Atmospheric Model Simulations for the 2003/04 Cold Season, *Journal of Climate*, 22(24), 6536–6560.
- Tang, X., F. Wang, Y. Chen, and M. Li (2009), Warming trend in northern East China Sea in recent four decades, *Chinese Journal of Oceanology and Limnology*, 27, 185–191.
- Taylor, K. E., V. Balaji, S. Hankin, M. Juckes, B. Lawrence, and S. Pascoe (2010), CMIP5 Data Reference SyntaxF (DRS) and Controlled Vocabularies.
- Taylor, K. E., R. J. Stouffer, and G. A. Meehl (2012), An overview of CMIP5 and the experiment design, *Bulletin of the American Meteorological Society*, 93(4), 485–498.
- Thompson, D. W., and S. Solomon (2002), Interpretation of recent Southern Hemisphere climate change, *Science*, 296(5569), 895–899.
- Thompson, D. W., and J. M. Wallace (2000), Annular modes in the extratropical circulation. Part I: month-to-month variability, *Journal of Climate*, 13(5), 1000–1016.
- Thompson, D. W., S. Solomon, P. J. Kushner, M. H. England, K. M. Grise, and D. J. Karoly (2011), Signatures of the antarctic ozone hole in southern hemisphere surface climate change, *Nature Geoscience*, 4(11), 741–749.
- Uppala, S. M., et al. (2005), The ERA-40 re-analysis, *Quarterly Journal of the Royal Meteorological Society*, 131(612), 2961–3012.
- Van de Poll, H., H. Grubb, and I. Astin (2006), Sampling uncertainty properties of cloud fraction estimates from random transect observations, *Journal of Geophysical Research:*

- 667 Atmospheres (1984–2012), 111(D22).
- 668 Wang, L., and W. Chen (2010), Downward Arctic Oscillation signal associated with
669 moderate weak stratospheric polar vortex and the cold December 2009, *Geophysical*
670 *Research Letters*, 37(9).
- 671 Wu, L., et al. (2012), Enhanced warming over the global subtropical western boundary
672 currents, *Nature Climate Change*, 2(3), 161–166.
- 673 Yang, H., J. Liu, G. Lohmann, X. Shi, Y. Hu, and X. Chen (2016), Ocean-atmosphere
674 dynamics changes associated with prominent ocean surface turbulent heat fluxes trends
675 during 1958–2013, *Ocean Dynamics*, 66(3), 353–365.
- 676 Yu, L., X. Jin, and R. A. Weller (2008), Multidecade Global Flux Datasets from the Ob-
677 jectively analyzed Air-sea Fluxes (OAFlux) Project: Latent and Sensible Heat Fluxes,
678 Ocean Evaporation, and Related Surface Meteorological Variables, *Tech. rep.*, OAFlux
679 Project Tech. Rep. OA-2008-01.